processes

MDPI

Article

Multi-Hazard Line Hardening with Equity Considerations: A Multi-Objective Optimization Framework

Ahmed Daeli [1,2] and Salman Mohagheghi [2,*]

[1] Electrical and Electronic Engineering Department, Jazan University, Jazan 45142, Saudi Arabia
[2] Electrical Engineering Department, Colorado School of Mines, Golden, CO 80401, USA
* Correspondence: smohaghe@mines.edu

Abstract

Climate change has increased the frequency and severity of extreme weather events such as wildfires, storms, high winds, and floods. Overhead lines are particularly vulnerable to these hazards, prompting utilities to consider reinforcement solutions through undergrounding overhead lines or structural hardening. However, these mitigation strategies are expensive and should be used selectively, prioritized for areas that are most at risk. This necessitates a framework to concurrently balance cost and resilience. In addition, the adopted reinforcement strategy must consider the consequences of possible outages on communities. This paper presents a multi-objective optimization framework to identify overhead line reinforcement strategies in a distribution system exposed to different hazards. A case study is presented for the city of Greeley, CO, which is prone to both wildfire and flood risks. Undergrounding overhead lines and reinforcing tower structures are considered as possible solutions for wildfire-prone areas and flood-prone areas, respectively. The proposed model is adaptable and can be applied to other hazard types and/or geographic regions. The proposed framework incorporates energy justice by prioritizing vulnerable populations and ensuring equitable distribution of reinforcement benefits. The results indicate that targeted hardening can reduce load shedding, improve outage response, and support equitable resilience planning.

Keywords: distribution system; energy justice; floods; infrastructural resilience; line hardening; resilience; social vulnerability; underground cables; wildfires

check for updates

Academic Editor: Ali S. Alghamdi

Received: 30 October 2025
Revised: 20 November 2025
Accepted: 27 November 2025
Published: 1 December 2025

Citation: Daeli, A.; Mohagheghi, S. Multi-Hazard Line Hardening with Equity Considerations: A Multi-Objective Optimization Framework. *Processes* **2025**, *13*, 3879. https://doi.org/10.3390/pr13123879

Copyright: © 2025 by the authors. Licensee MDPI, Basel, Switzerland. This article is an open access article distributed under the terms and conditions of the Creative Commons Attribution (CC BY) license (https://creativecommons.org/licenses/by/4.0/).

1. Introduction

Over the past two decades, the vulnerability of electric power systems to extreme weather events has become increasingly evident. Natural disasters such as wildfires, floods, hurricanes, and severe storms have grown in both frequency and intensity due to the changing climate. Distribution systems, which represent the final and most exposed layer of the power grid, are particularly at risk due to their wider geographical dispersion. While these systems are designed to manage normal operational stresses such as equipment failures and localized outages, they are not built to withstand large-scale natural disasters. The difference is significant: minor disturbances can usually be repaired within a few hours, whereas extreme weather events can damage a large number of components at once, leaving entire communities without power for days or even weeks.

Recent events continue to highlight how extreme weather directly exposes weaknesses in distribution networks. The 2021 Texas winter storm left millions without power for days, resulting in more than 200 deaths and widespread losses in water, heating, and medical

services [1]. Similar cascading outages were observed during Hurricane Ian in 2022, where high winds and flooding damaged distribution components across several states [2]. The 2021 Marshall Fire in Colorado also stressed overhead distribution lines under extreme wind and wildfire conditions [3]. The statistics from past events highlight the severity of this problem. Between 2000 and 2021, weather-related events were responsible for roughly 83% of all major outages in the United States, and since 2011 the frequency of outages linked to extreme weather has increased by almost 80% [4]. These patterns accelerated national and state policies that encourage risk-based reinforcement and equity-aware resilience planning, especially for vulnerable communities who often experience slower recovery and longer outage durations. Events of this type fall under what researchers classify as high-impact low-probability (HILP). Although relatively rare, their impact is disproportionate, disrupting not only electricity supply but also public safety, economic activity, and essential services such as hospitals, water systems, and emergency response facilities. Traditional reliability-based planning frameworks are insufficient in this context. Metrics such as SAIDI and SAIFI, while useful for measuring average performance under normal conditions, cannot represent the scale, duration, and societal consequences of long-duration, widespread outages caused by extreme weather events and natural hazards.

To address this shortcoming, utilities and researchers have increasingly turned to the concept of resilience. Unlike reliability, which emphasizes continuity of service under routine conditions, resilience considers the ability of the system to prepare for, withstand, adapt to, and recover from extraordinary disruptions. The U.S. Federal Energy Regulatory Commission (FERC) defines resilience as "the ability to withstand and reduce the magnitude and/or duration of disruptive events, which includes the capability to anticipate, absorb, adapt to, and/or rapidly recover from such an event" [5]. Similarly, the National Infrastructure Advisory Council (NIAC) highlights four attributes of robustness, resourcefulness, adaptability, and rapidity to describe how infrastructure systems should respond to major disruptions [6]. Together, these definitions make it clear that resilience is a multidimensional attribute.

In practice, resilience strategies for distribution systems are often categorized as preventive, corrective, or restorative measures. Preventive measures are applied before events occur. Specific to distribution systems, they may include vegetation management, replacement of wooden poles with steel or concrete ones, undergrounding of overhead lines, or reinforcement of tower foundations in flood-prone regions. Corrective measures are activated as events unfold and may include operational adjustments such as feeder reconfiguration or the use of mobile generators to maintain supply for critical loads. Finally, restorative measures take place after the event has ended and are focused on repairing damaged assets and restoring power to the affected areas. Although these categories are distinct, they are highly interdependent. Preventive measures, in particular, have the greatest long-term impact because they reduce the overall vulnerability of the system and in turn, improve the effectiveness of corrective and restorative actions [7].

In recent years, optimization models have become the dominant tool for planning resilience strategies. These models allow utilities to evaluate different combinations of hardening measures, distributed energy resource (DER) placement, storage allocation, and operational strategies under budgetary and operational constraints. Objective functions vary depending on the focus of the study. Some models aim to minimize load curtailment [8,9], while others minimize the economic cost of unserved demand [10], or balance investment costs against improvements in resilience [11]. More recent studies use multi-objective formulations that capture trade-offs between technical resilience, economic performance, and social welfare [12,13].

The treatment of uncertainty is another distinguishing factor in resilience optimization. Deterministic models evaluate resilience for specific hazard scenarios or single networks, making them useful for case-specific planning [14]. Stochastic optimization, on the other hand, captures the probabilistic nature of hazards by incorporating multiple scenarios with associated probabilities [15,16]. Alternatively, robust optimization focuses on worst-case conditions, ensuring acceptable performance under the most damaging scenarios [17–19]. Hybrid approaches have also been developed, combining stochastic and robust methods to balance expected performance with worst-case conditions. All these models are constrained by typical system constraints, including but not limited to radiality in configuration, nodal power balance, voltage limits, thermal rating limits, and budget allocations [20,21].

Among the many resilience strategies considered, line hardening has consistently emerged as one of the most effective and widely studied. For wildfire-prone regions, undergrounding overhead lines is the preferred option since it eliminates direct exposure to fire or the resulting heat. However, it is extremely costly and, more importantly, not suitable for all hazards. For instance, in flood-prone areas, underground cables may be at risk of water ingress and hence, more costly maintenance. For floods, utilities instead turn to structural hardening strategies such as elevating poles, using steel or concrete materials, and/or reinforcing foundations against erosion and submersion. For hurricanes and severe wind events, line hardening typically involves upgrading pole classes, reinforcing conductors, or selectively undergrounding critical segments. While the literature on line hardening is extensive, most studies focus on a single hazard type. As a result, their applicability remains limited in regions where multiple hazards overlap.

To provide a clear picture of the existing research on this topic, Table 1 summarizes recent optimization-based studies that explicitly include line hardening. Each study is characterized by its objective function, decision variables, constraints, resilience metrics, case study system, optimization type, and hazard type.

Table 1. Summary of optimization models for distribution network resilience. Abbreviations: ENS—Energy Not Supplied; DG—Distributed Generation; ESS—Energy Storage System; O&M—Operation and Maintenance; IGDT—Information Gap Decision Theory; GA—Genetic Algorithm; MILP—Mixed-Integer Linear Programming; DLR—Dynamic Line Rating; Interdep.—Interdependency; Stoch.—Stochastic; Determ.—Deterministic; Restor.—Restoration; sw.—Switches.

Ref.	Objective Function	Decision Variables	Constraints	Resilience Metric	Case Study	Optimization Type	Hazard
[22]	Min. ENS cost	Line hardening	Budget, radiality	ENS cost	IEEE 33-bus	Stoch. + GA	Hurricane
[18]	Min. invest. + outage cost	Harden lines, DG, mob. gen.	Budget, power flow	Exp. post-event cost	IEEE 33-bus	Stoch. MILP	Typhoon
[19]	Min. total cost	Line hard., DG, ESS, sw.	Gas–power coupling, Budget	Worst-case ENS	Coupled IEEE 33-bus + gas	Stoch. + robust	Multi-hazard
[23]	Min. invest. + O&M + outage	Harden lines, DG, reconfig.	Budget, IGDT	ENS (worst-case)	IEEE 33-bus	Hybrid	Hurricane
[13]	Max. restored service	Power + water hardening	Interdep., budget	% service maintained	Guayama, Puerto Rico	Stochastic	Hurricane
[14]	Min. total cost	Undergrounding, poles, Vegetation	Budget, fire model	Lines intact, load served	IEEE 15-bus	Determ. MILP	Wildfire
[24]	Min. worst-case load shed	Harden lines, DG siting	Budget	Worst-case load served	IEEE feeder	Robust	General disasters
[25]	Multi-obj.: cost, shed, emissions	Harden lines vs. DLR	AC flow, Pareto	Resilience index	IEEE 24-bus	Multi-objective	Extreme
[26]	Min. invest. + ENS	Harden lines, DG, sw.	Budget, dust fragility	ENS	IEEE feeder	Stochastic	Dust storms
[27]	Min. cost + load shed	Line hard., gas DG, ESS	Gas–power constr.	ENS	IEEE 118-bus + gas	Two-stage stoch.	Hurricanes
[16]	Min. invest. + ENS + repair	Harden lines, DG, sw.	Spatio-temp. fragility	ENS + repair	IEEE 123-bus	Two-stage MILP	Hurricanes
[15]	Min. invest + ENS	Harden lines, DG, sw.	Fragility-based	ENS + cost	IEEE 34/123-bus	Two-stage MILP	Extreme

Table 1. *Cont.*

Ref.	Objective Function	Decision Variables	Constraints	Resilience Metric	Case Study	Optimization Type	Hazard
[17]	Min. shed + traffic delay	Harden lines, DG	Power + traffic flow	Load + travel time	IEEE 33-bus + traffic	Robust tri-level	Natural disasters
[28]	Min. weighted shed	Harden lines, ESS	Budget	% load	IEEE 33-node + real grid	Robust D–A–D	Natural disasters
[12]	Max. social welfare	Upgrading Poles, DG	Budget, balance	Social welfare	IEEE 33-bus	Stochastic	Hurricane

This paper extends the authors' previous work on power grid infrastructural resilience [29], which focused on mitigating wildfire risks in distribution systems. Building on that foundation, this study introduces a hybrid mitigation strategy designed to address multiple hazards, namely, wildfires and floods. The proposed approach integrates resilience, cost, and energy justice considerations when optimizing the allocation of resources in the study area. Line undergrounding is assumed to be the strategy of choice in wildfire-prone regions to mitigate fire-related risks, while flood-prone areas are considered as candidates for structural reinforcement such as elevating pole heights, installing steel or concrete poles, and strengthening foundations to resist water ingress and erosion. These hybrid strategies provide a tailored response to the diverse environmental hazards faced by the power grid, enhancing overall system resilience and adaptability. The optimization model proposed in this paper is intended for the planning stage, i.e., can be performed based on the available data related to the nature and severity of natural hazards within a geographical area before those hazards turn into disasters. Beyond technical aspects, this study incorporates sociotechnical perspectives by prioritizing vulnerable populations who may be disproportionately affected by the consequences of outages, ensuring that those most at risk are assigned higher priority for targeted resilience improvements. The study also ensures that the allocation of both the benefits and costs of grid reinforcement across all service areas are equitable, preventing disproportionate burdens on specific communities. The key contributions of this paper are as follows:

- Multi-Hazard Resilience Framework: Unlike the authors' previous work that focused solely on wildfire risks, this study introduces a dual-hazard approach by incorporating flood-hardening strategies, ensuring a more comprehensive and adaptable grid reinforcement plan. The proposed model is scalable and upon need, can be expanded to include other types of hazards and hazard mitigation strategies.
- Enhanced Objective Functions: Objective functions are introduced related to outage duration and scope. Not only does the model minimize total load shedding but it also ensures that the worst-impacted regions do not experience disproportionate outage durations or severity.
- Social Vulnerability Informed Analysis: To quantify the consequences of outages, the model incorporates a social vulnerability index (SVI) for long-duration power outages [30], ensuring that grid resilience investments prioritize communities most negatively affected by the consequences of power disruptions.
- Equitable Distribution of Reinforcement Benefits: The model also enforces distributional justice, ensuring that resilience improvements are evenly distributed across the network. This prevents scenarios where some areas receive disproportionate investment while others remain vulnerable.

The remainder of the paper is organized as follows: Section 2 presents the problem formulation and methodology, detailing the integration of resilience, cost, and energy justice objectives into a hybrid mitigation framework. Section 3 describes a detailed case study that evaluates the effectiveness of the proposed strategies in a region exposed to both wildfire and flood risks. Section 4 showcases the results, validating the proposed

model and its ability to balance resilience and justice considerations effectively. Finally, Section 5 of the paper provides concluding remarks and outlines potential future directions for advancing power grid resilience in multi-risk environments.

2. Problem Formulation

2.1. Objective Functions

The optimization model aims to enhance power system resilience while ensuring equity and cost efficiency. To achieve this, several objectives are formulated within a multi-objective optimization framework, as outlined below.

2.1.1. Maximize Recognition Justice

Recognition justice in power grid resilience ensures that the needs of socially vulnerable communities are acknowledged and prioritized in resilience planning. This is accomplished by incorporating social vulnerability levels of demand nodes into the optimization framework. During extreme weather events, maintaining electricity supply is critical to minimizing the adverse effects on affected communities. Objective function (1) addresses this by minimizing the load not served (LNS) across all risk scenarios and contingencies in the scenario set H and S, while weighting the unserved load based on the social vulnerability of each demand node. This formulation recognizes that prolonged power outages have disproportionate impacts on different communities, particularly those with heightened vulnerabilities, as disruptions to electricity access can significantly threaten lives and livelihoods [30]. By integrating social vulnerability as a weighting factor, this objective aligns with the principles of recognition justice, ensuring that the most at-risk populations receive priority in restoration efforts. Objective function (2) seeks to minimize the total number of time steps in which a demand node experiences power curtailment. This objective ensures that outages are not only reduced in magnitude but also in duration, thereby improving service availability for all customers. By considering both the severity of unserved load and the duration of outages, the optimization framework promotes equitable distribution of electricity supply during contingencies.

$$\min \sum_{h\in H}\sum_{s\in S} p_{h,s} \sum_{i\in D}\sum_{t\in T} \mathrm{SV}_d (P^d_{i,t} - p^d_{i,t,h,s}) \tag{1}$$

$$\min \sum_{h\in H}\sum_{s\in S} p_{h,s} \sum_{i\in D}\sum_{t\in T} \mathrm{SV}_d \cdot m_{i,t,h,s} \tag{2}$$

2.1.2. Minimize Cost

A fundamental consideration in power grid resilience planning is the financial feasibility of implementing infrastructure improvements. The cost of reinforcing power lines to enhance resilience must be minimized as shown in Objective (3). The cost of line renewal, which includes undergrounding and structural reinforcement, is assumed in this study to be linearly proportional to the length of the line and independent of its location. This assumption simplifies the optimization model while maintaining its general applicability. However, in practical scenarios, line renewal costs may vary due to factors such as terrain complexity, land acquisition costs, and regulatory constraints. Further, factors such as costs across the entire life cycle of the line, environmental impacts, maintenance costs, and/or the impacts on land value may be incorporated into the cost term.

$$\min \sum_{h\in H}\sum_{(i,j)\in L_v} u_{i,j,h}\, l_{i,j}\, c_h \tag{3}$$

2.1.3. Maximize Distributional Justice

Distributional justice in grid reinforcement ensures that both the benefits and costs of infrastructure hardening are equitably distributed across all customers. Since the financial burden of reinforcement projects, such as undergrounding lines or strengthening poles and towers, is ultimately reflected in electricity rates for everyone, it is essential to ensure that reliability improvements are not concentrated in specific areas while others remain vulnerable to prolonged outages. To achieve this, distributional justice is quantified in this study through multiple objective functions. The first objective minimizes the variance in the percentage of load loss across all scenarios and demand nodes, as formulated in Objective (4). This objective function ensures that no particular group of customers disproportionately experiences power interruptions and is therefore considered in this paper as a measure of energy access equity across the system, referred to as equity index. Additionally, Objective (5) minimizes the maximum deviations in supplied demand, effectively addressing outliers in load reduction percentages across all nodes and time steps. This prevents significant disparities in power availability among different customers. Objective (6) minimizes inconsistencies in the number of time steps during which a demand node experiences partial load curtailment, ensuring a more uniform distribution of outage durations. Unlike recognition justice, where outage impacts are weighted based on social vulnerability levels, distributional justice ensures that all customers are treated equally in terms of resilience benefits. This approach prevents certain groups from experiencing disproportionately severe outages while others recover more quickly, promoting a balanced and equitable power system resilience strategy.

$$\min \sum_{h\in H}\sum_{s\in S} p_{h,s} \sum_{i\in D}\sum_{t\in T}\left(\frac{P^d_{i,t} - p^d_{i,t,h,s}}{P^d_{i,t}}\right)^2 \tag{4}$$

$$\min \max_{(i,t)} \sum_{h\in H}\sum_{s\in S} p_{h,s}\left(\frac{P^d_{i,t} - p^d_{i,t,h,s}}{P^d_{i,t}}\right) \tag{5}$$

$$\min \max_{i} \sum_{h\in H}\sum_{s\in S} p_{h,s} \sum_{t\in T} m_{i,t,h,s} \tag{6}$$

2.2. Constraints

The above objective functions are solved subject to the following constraints:

2.2.1. Node Power Flow Constraints

At each node, total generation minus total demand equals the sum of powers flowing outwards through the lines connected to that node. This constraint is enforced for all customers, at every time step and under each scenario, as shown in (7). Since the proposed model is intended for the planning stage, the nodal demand values can be thought of as average hourly demand that are known a priori based on historical data.

$$\forall\, i\in N,\ t\in T,\ h\in H,\ s\in S: \quad p^g_{i,t,h,s} - p^d_{i,t,h,s} = \sum_{\substack{j\in N\\ j\neq i}} p_{i,j,t,h,s} \tag{7}$$

2.2.2. Line Flows

Power flows through lines are modeled using DC power flow. This constraint consists of two sets, one for lines that are robust (not vulnerable) against the contingencies under study and another for vulnerable lines that are candidates for hardening. Equation (8) is bilinear but is reformulated using the Big-K formulation proposed in [31], as shown in (9). Here, K is a large positive constant. When the status variable of a line is 1, the power

flowing through the line equals the susceptance multiplied by the voltage angle difference across that line (based on DC power flow) as each side of the equality constraint must equal zero. When the status variable is zero, the power flow through the line (which is not operational) is constrained to be zero. Equation (10) ensures that the overall status of the line is determined by a combination of its vulnerability to a particular scenario and whether it is hardened. A line is assumed unavailable during a scenario if it is vulnerable and not reinforced.

$$\forall\,(i,j)\in L,\ \forall t\in T,\ \forall h\in H,\ \forall s\in S:\quad \frac{p_{i,j,t,h,s}}{S_{\text{base}}}=\frac{b_{i,j}}{Y_{\text{base}}}s_{i,j,h,s}(\delta_{i,t,h,s}-\delta_{j,t,h,s}) \tag{8}$$

$$\begin{aligned}\forall(i,j)\in L,\forall t\in T,\forall h\in H,\forall s\in S:\\ -(1-s_{i,j,h,s})K\le\frac{p_{i,j,t,h,s}}{S_{\text{base}}}-\frac{b_{i,j}}{Y_{\text{base}}}(\delta_{i,t,h,s}-\delta_{j,t,h,s})\\ \le(1-s_{i,j,h,s})K\end{aligned} \tag{9}$$

$$\forall\,(i,j)\in L,\ \forall h\in H,\ \forall s\in S:\quad s_{i,j,h,s}=\min\left[1,\ v_{i,j,h,s}+u_{i,j,h}\right] \tag{10}$$

2.2.3. Line Power Flow Limits

Two sets of equations are defined for lines that are robust against the contingencies under study and vulnerable lines that are candidates for hardening. Note that in (12), the power through a vulnerable line is zero unless it is hardened. This is ensured by multiplying the upper and lower limits by $s_{i,j,h}$.

$$\forall\,(i,j)\in L\setminus L_v,\ \forall\,t\in T,\ \forall\,h\in H,\ \forall\,s\in S:\quad -\overline{P}_{i,j,t}\le p_{i,j,t,h,s}\le\overline{P}_{i,j,t} \tag{11}$$

$$\forall\,(i,j)\in L_v,\ \forall\,t\in T,\ \forall\,h\in H,\ \forall\,s\in S:\quad -\overline{P}_{i,j,t}\cdot s_{i,j,h,s}\le p_{i,j,t,h,s}\le\overline{P}_{i,j,t}\cdot s_{i,j,h,s} \tag{12}$$

2.2.4. Generation Limits

Power produced by generation units (including distributed energy resources and the main distribution substation) is constrained by the applicable upper and lower limits.

$$\forall\,i\in G,\ \forall\,t\in T,\ \forall\,h\in H,\ \forall\,s\in S:\quad -\underline{P}^{g}_{i,t}\le p^{g}_{i,t,h,s}\le\overline{P}^{g}_{i,t} \tag{13}$$

2.2.5. Demand Limits

Power supplied to demand nodes should not exceed the desired values, as shown in (14). To indicate whether a demand node is experiencing full or partial demand reduction, two auxiliary binary variables are introduced in (15) and (16) to indicate if the demand is met. Here, M is a large positive number and ϵ is a small positive number. If power supplied to demand node i is less than the desired value under a scenario s for hazard h, Equation (15) ensures that auxiliary variable $m_{i,t,h,s}$ is 1. On the other hand, if the demand node receives the desired demand, Equation (16) sets $n_{i,t,h,s}$ to 1. Equation (17) will then ensure that these two auxiliary variables cannot both be 1 at the same time.

$$\forall\,i\in D,\ \forall\,t\in T,\ \forall\,h\in H,\ \forall\,s\in S:\quad 0\le p^{d}_{i,t,h,s}\le P^{d}_{i,t} \tag{14}$$

$$\forall\,i\in D,\ \forall\,t\in T,\ \forall\,h\in H,\ \forall\,s\in S:\quad (P^{d}_{i,t}-p^{d}_{i,t,h,s})-M\cdot m_{i,t,h,s}\le 0 \tag{15}$$

$$\forall\,i\in D,\ \forall\,t\in T,\ \forall\,h\in H,\ \forall\,s\in S:\quad (P^{d}_{i,t}-p^{d}_{i,t,h,s})+M\cdot n_{i,t,h,s}\ge\epsilon \tag{16}$$

$$\forall\,i\in D,\ \forall\,t\in T,\ \forall\,h\in H,\ \forall\,s\in S:\quad m_{i,t,h,s}+n_{i,t,h,s}=1 \tag{17}$$

2.2.6. Line Renewal Constraints

In the most general case, it is possible for a particular line reinforcement strategy to serve multiple hazard types. However, in this study, it is assumed that different reinforcement strategies are adopted for different hazards, for instance, undergrounding lines for resilience against wildfires and hardening towers and/or the tower foundation for resilience against flooding events. Under this assumption, only one reinforcement strategy can be implemented for each line, as indicated in Equation (18).

$$\forall (i,j) \in L : \sum_{h \in H} u_{i,j,h} \leq 1 \tag{18}$$

2.2.7. Node Constraints

Node voltage phase angles are limited to a specific range as shown below.

$$\forall\, i \in N,\ \forall\, t \in T,\ \forall\, h \in H,\ \forall\, s \in S : \quad -\bar{\delta} \leq \delta_{i,t,h,s} \leq \bar{\delta} \tag{19}$$

2.3. Methodology

The optimization model consists of Objectives (1)–(6) subject to Constraints (7)–(19). A Chebyshev goal programming approach [32] is adopted because it facilitates striking a balance between different objective functions without artificially favoring one over the others. In modeling the problem, each objective function is initially assigned a target (goal) value. These targets represent the desired outcomes within the multi-objective context. Given the potential contradiction among objectives, it is expected that achieving their global optima simultaneously may not always be feasible. To address this, each objective function is allowed to deviate from its target value, i.e., true optimal value. The goal of the optimization model is then to simultaneously minimize those deviations (deficiencies) compared to their corresponding single objective optima. The overall problem formulation is then expressed as follows:

$$\min Q \tag{20}$$

Subject to the following:

$$\forall f : O_f - b_f \leq T_f \tag{21}$$

$$\frac{b_f}{T_f} \leq Q \tag{22}$$

$$b_f \geq 0 \tag{23}$$

Constraint (20) presents the linear objective function, aiming to minimize the maximum deviation among all objectives. Constraint (21) introduces a deficiency variable for each objective function, converting the constraints from hard to soft. As the units for each objective differ, the deficiency variables are normalized based on their respective target values. Additionally, a variable Q is defined as the upper bound for the normalized deficiency variables, as depicted in Constraint (22).

The proposed model does not introduce a new optimization technique. Instead, it adapts a well-established multi-objective formulation and integrates equity-driven metrics directly into the decision process. The novelty lies in how we embed recognition and distributional justice within line-hardening decisions, providing a practical framework that utilities can directly implement without requiring algorithmic complexity.

3. Case Study

3.1. System Description

The test system used in this study is based on a realistic radial distribution network serving the cities of Greeley and Eaton in Weld County, Colorado [33]. This region provides a meaningful testbed because it combines urban and semi-rural demand centers with exposure to multiple hazards, i.e., wildfires and flooding. The modeled system includes 2 substations (buses 79 and 80), 8 distribution feeders, 78 demand buses, and 77 line segments, supplying power to roughly 30,000 residential customers. The system peak load is estimated at 60 MW, with demand profiles calibrated against residential electricity consumption data for Colorado households [34]. Figure 1 illustrates the average hourly residential demand profile, which serves as the baseline for quantifying individual demand nodes.

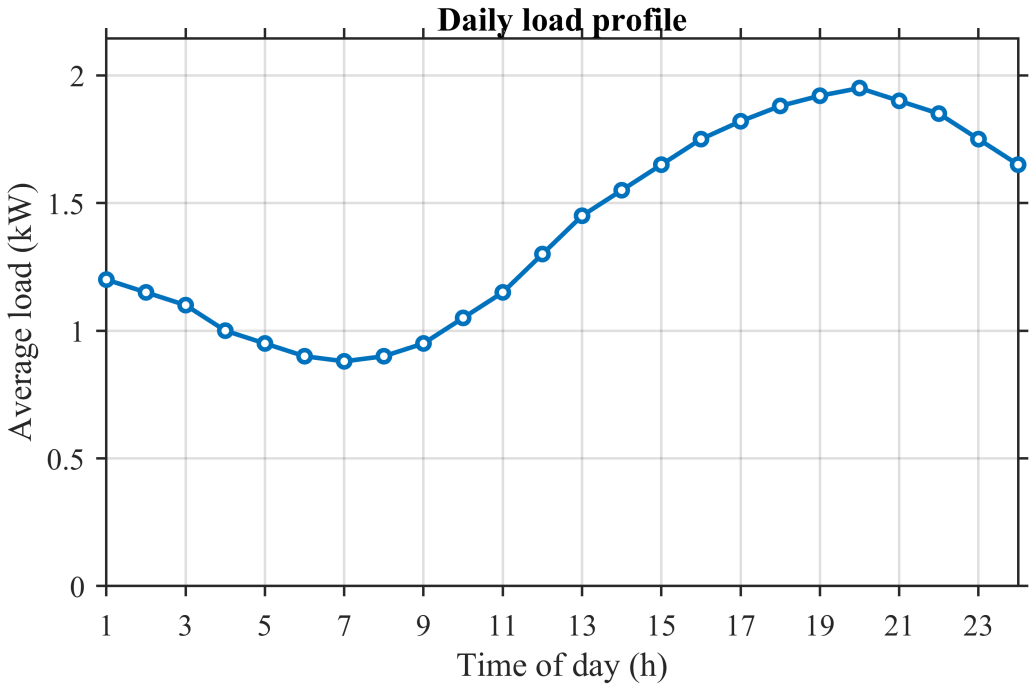


Figure 1. Average hourly household demand profile, generated using data provided in [29].

The conductor types used across feeders are representative of typical rural-urban mixed systems. The primary feeders in Greeley, labeled GRLY-1001 through GRLY-1005, are assumed to use 795 AAC (all-aluminum conductor), reflecting higher-capacity designs for larger load centers. Smaller feeders, such as GRLY-1006, are modeled with 336 ACSR (aluminum conductor steel-reinforced), while the Eaton feeder is modeled with 556 ACSR, reflecting its intermediate load characteristics. The nominal operating voltage of the network is 12.47 kV, which is consistent with regional distribution practice.

For resilience planning, reinforcement costs are critical. The cost of converting overhead distribution lines to underground cable is estimated at 3 million USD per mile, while the cost of flood hardening overhead lines (e.g., replacing wooden poles with steel or concrete, elevating pole heights, and reinforcing foundations against water damage) is approximated at 200,000 USD per mile. These values are consistent with cost benchmarks reported for U.S. distribution systems in [35]. Although approximate, they provide a reasonable basis for planning-level optimization. All cost values are expressed in 2020 USD.

To capture the social dimension of resilience, each demand node is assigned a Social Vulnerability Index (SVI) score based on the data provided in [30], where vulnerability indicators (i.e., health, preparedness, and evacuation) were normalized and a final score

was obtained for each tract using Pareto ranking to avoid introducing subjective weights. In the model, each node inherits the score of the census tract in which it is located, allowing the optimization model to prioritize lines that serve communities with higher vulnerability. These vulnerability values range from 0 (least vulnerable) to 1 (most vulnerable).

Figure 2 shows the overlay of social vulnerability with the test system. In cases where census data are unavailable, such as the University of Northern Colorado campus (low residential population), an index of 0 is assigned. Both substations are also assigned a score of 0, since they do not directly represent any residential demand.

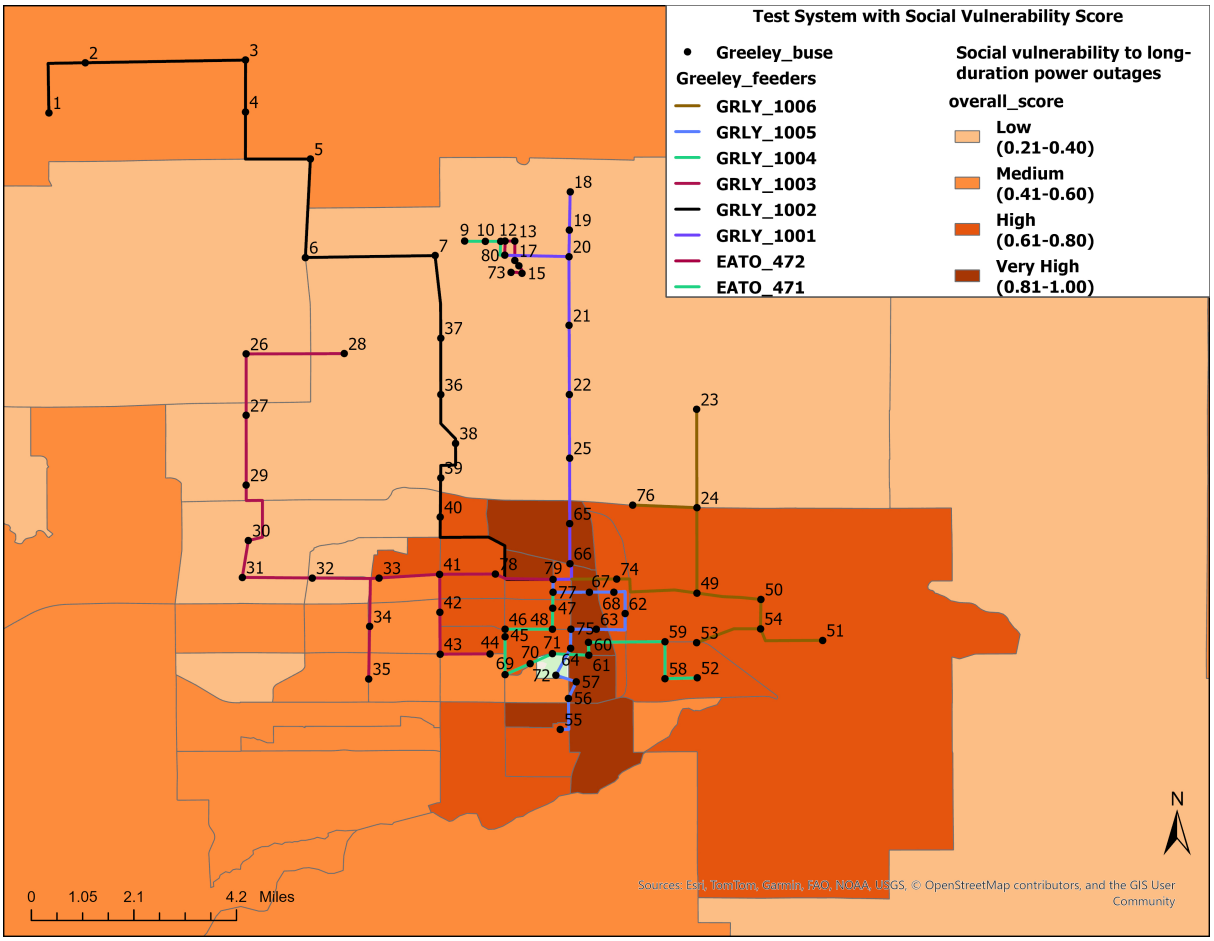


Figure 2. Overlay of social vulnerability indices with the test system (feeders and buses), generated using data from [29,30].

This integration of physical infrastructure with social vulnerability provides a richer framework for evaluating not just technical system performance, but also the equity implications of resilience planning.

3.2. Scenario Development

To evaluate resilience under multi-hazard conditions, contingency scenarios were developed for wildfires and flooding, which represent two of the most pressing hazards in northern Colorado.

3.2.1. Wildfire Scenarios

Wildfire risk was assessed using burn probability maps published by the USDA Forest Service [36]. Burn probability, expressed as a percentage, is defined as the likelihood that a wildfire will occur at a given location. In this study, any line segment with a burn probability of 0.1% or higher (equivalent to 1 in 1000) was considered at risk. For each

wildfire scenario, the probability of occurrence was calculated by averaging the burn probabilities of the affected line segments, with the maximum probability along each line serving as the reference value.

The wildfire risk was divided into three geographical clusters (A1, A2, A3), each forming a distinct contingency scenario. This division reflects the spatial correlation of wildfire events, where adjacent lines are likely to be simultaneously exposed to fire. Figure 3 shows the burn probability distribution across the study area and highlights the lines included in each scenario.

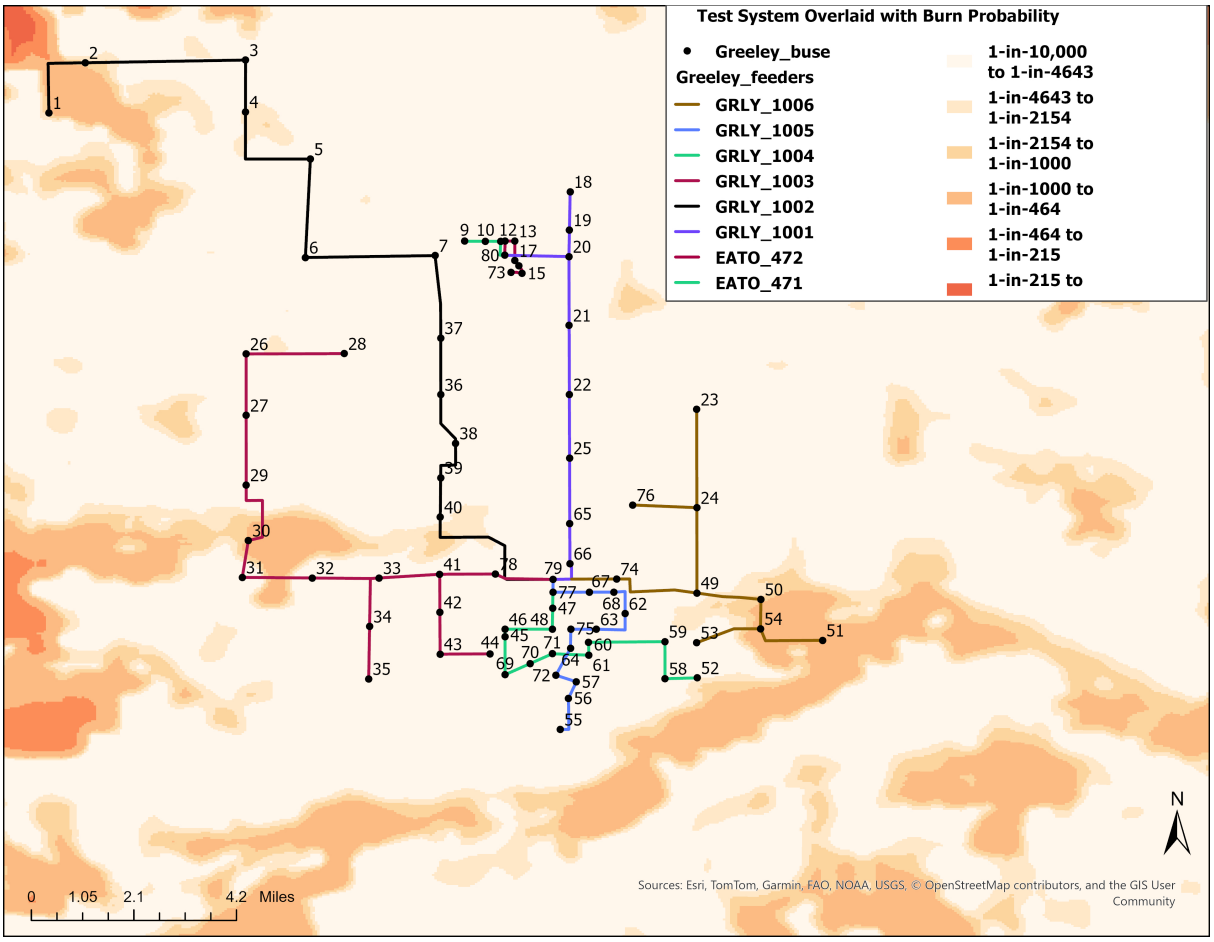


Figure 3. Burn probability overlaid with the test system, including feeders and buses, generated using data from [29].

3.2.2. Flood Scenario

Flood exposure was assessed using the 100-year floodplain maps for Weld County, CO, available through the county property portal [37]. The 100-year floodplain is defined as the area with a 1% annual probability of flooding, which aligns with standard risk metrics used in hazard planning. Any line segment within this floodplain was classified as vulnerable and included in the flood scenario. The probability of the flood contingency scenario was therefore set to 1%, consistent with the event definition. Figure 4 shows the flood-prone areas of the test system, with affected lines identified.

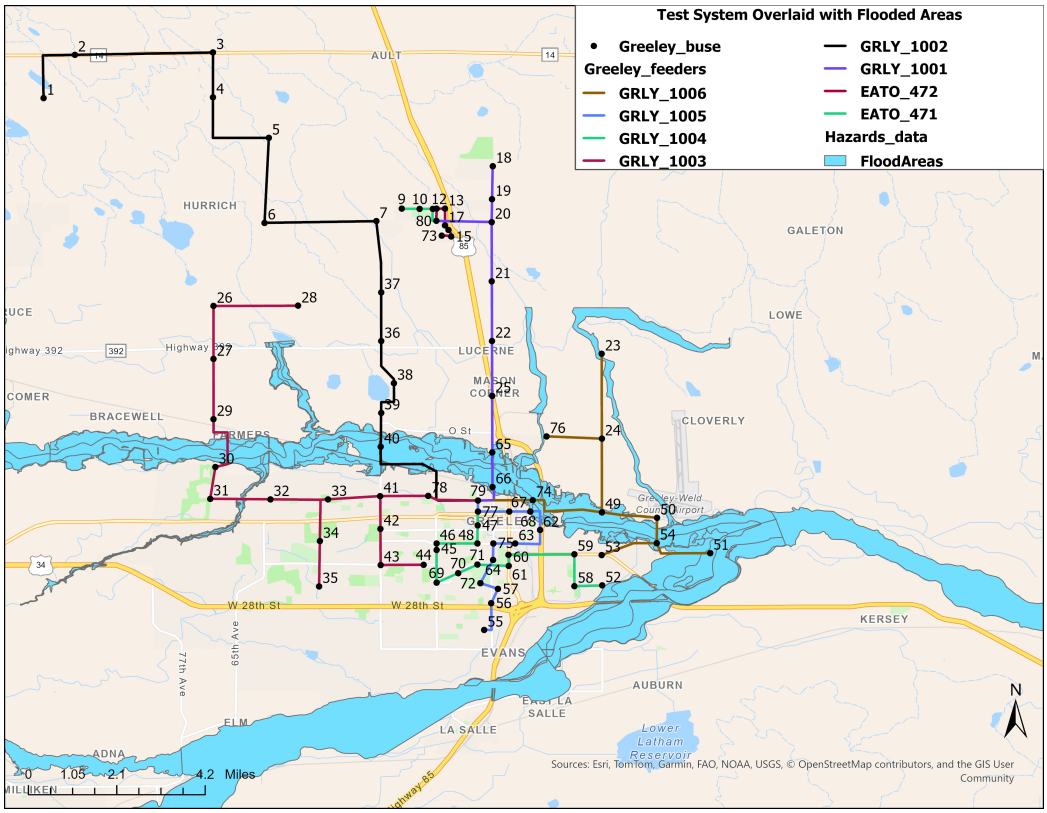


Figure 4. The 100-year floodplain probability overlaid with the test system, including feeders and buses.

3.2.3. Multi-Hazard Representation

Combining wildfire and flood risks yields a set of four scenarios that collectively represent the hazard exposure of the system. Scenarios 1 through 3 capture wildfire risks in areas A1, A2, and A3, while Scenario 4 captures flood exposure. These scenarios are summarized in Table 2, including the description, affected lines, and associated probabilities of occurrence.

Table 2. Scenario description and affected lines.

Scenario	Description	Affected Lines	Prob. (%)
1	Wildfire (A1)	L30-29, L26-28, L32-31, L31-30	0.60
2	Wildfire (A2)	L3-2, L5-4, L2-1	1.21
3	Wildfire (A3)	L79-40, L54-51, L54-53, L49-50, L50-54	1.14
4	Flood (100-yr)	L50-54, L74-49, L66-65, L79-40, L30-29	1.00

This structured scenario development enables a comprehensive multi-hazard assessment of resilience. By evaluating wildfire and flood risks within the same framework, the case study captures the need for hybrid reinforcement strategies. For instance, undergrounding is highly effective in wildfire-prone areas but unsuitable in flood zones, while pole hardening performs well against flooding but offers limited protection from wildfire exposure. These scenarios highlight the practical trade-offs utilities face when planning for resilience in regions exposed to multiple hazards.

When a line segment is exposed to hazards that require different hardening measures (for example, elevation for floods versus undergrounding for wildfires), the model evaluates each option independently and selects the one that yields the best overall performance. Because cost, resilience benefits, and equity are optimized together, the solution naturally balances these objectives rather than enforcing a predefined hierarchy of decisions.

4. Results and Discussion

The optimization framework was modeled as minimize (20), subject to (1)–(19) and (21)–(23) in AMPL [38] and solved using Gurobi version 10.0 [39] on a server equipped with two Intel Xeon E5620 processors (2.4 GHz) and 48 GB of RAM, running Ubuntu version 22.04.2 (Intel Corporation, Santa Clara, CA, USA).The model demonstrated high computational efficiency, achieving convergence within 5 s. This rapid runtime is primarily due to the planning-stage nature of the model, where detailed operational constraints (e.g., voltage drops, reactive power, dynamic load behaviors) are typically excluded to improve computational efficiency when considering and comparing various design scenarios and options. Despite its efficiency on the test system, the framework is scalable and generalizable to larger distribution networks. Its modular structure allows for the addition of more objectives, scenarios, or network components with minimal restructuring. For larger systems, decomposition strategies or parallel computing could be employed to maintain runtime efficiency. These features make the model suitable for both targeted planning studies and broader utility-wide reinforcement strategies. To apply the Chebyshev goal programming approach, each objective function was first solved independently to determine its global optimal value. These optimal values were then used as the target values for the multi-objective framework. As expected, solving for each objective function in isolation resulted in single-objective optima of zero. This is due to the nature of the problem: if cost minimization is not enforced, all vulnerable lines are reinforced, eliminating load shedding (LNS) under all contingencies, and consequently yielding zero for Objectives (1), (2), (4), (5), and (6). Conversely, if LNS minimization is not enforced, no lines are reinforced, resulting in zero cost. However, when all objectives are considered simultaneously, none of these optimal values can be fully attained due to their inherent trade-offs.

The Chebyshev goal programming methodology ensures a balanced optimization process by preventing any single objective from dominating the others. To address potential denominator issues inherent in this approach, the target values for each objective were adjusted slightly above zero, ensuring numerical stability while maintaining optimization accuracy. Table 3 presents a comparison of the results obtained from both single-objective and multi-objective optimization models, demonstrating how the proposed framework simultaneously optimizes multiple conflicting criteria.

Table 3. Optimal values for single- and multi-objective models.

Objective Function	Single Optima	Multi-Obj Optima
Weighted load not served LNS (kW)	0	329.5
Weighted total number of outage time steps	0	2.1488
Cost (USD)	0	$13.55 M
Variance of load lost (%)	0	5.10568
Outlier of load lost (%)	0	0.012
Outlier of outage time steps	0	5.2146

To assess the impact of energy justice considerations in distribution network reinforcement, three distinct optimization cases were analyzed, each exploring the trade-offs between minimizing total load shedding (LNS), reducing costs, and ensuring equitable power restoration across the network.

- Case 1 incorporates all objective functions, including recognition justice, distributional justice, and cost optimization, ensuring a balanced approach to resilience planning.
- Case 2 removes recognition justice, prioritizing cost reduction and minimizing load shedding while maintaining distributional justice.

- Case 3 excludes both recognition and distributional justice, focusing solely on minimizing LNS and cost, without considering equity in service restoration.

Table 4 summarizes the results, highlighting the effects of each case on cost efficiency, resilience, and equity in grid reinforcement decisions.

Table 4. Comparison of different cases for grid resilience.

Metric	Case 1 (All Objectives)	Case 2 (Energy Justice & Cost)	Case 3 (LNS & Cost)
Total load shedding (kW)	843.5	680.8	655
Weighted load shedding (kW)	329.5	271.5	264.6
Cost (USD)	13,554,000	28,104,000	27,134,000
Equity index	5.1	4.3	4.6
Avg. outage time (h)	2.15	1.9	16.1
Lines reinforced	L5-4, L30-29, L32-31, L49-50, L50-54, L74-49, L70-40	L2-1, L3-2, L5-4, L30-29, L31-30, L32-31, L49-50, L50-54, L74-49, L79-40	L5-4, L30-29, L31-30, L32-31, L49-50, L50-54, L54-53, L74-49, L79-40
Most nodes with high load shedding	1, 2, 3, 28, 26, 51, 53	28, 26, 54, 51, 53	1, 2, 3, 26, 27, 28, 51, 53

In Case 1, the optimization framework integrates both recognition justice and distributional justice, alongside cost minimization. Recognition justice ensures that load shedding and outage duration are weighted based on the social vulnerability (SV) index of each demand node, prioritizing power restoration for the most vulnerable customers. Additionally, distributional justice ensures that load shedding and outage durations are distributed more equitably, preventing certain groups from disproportionately experiencing prolonged outages. The results indicate a total load shedding of 843.5 kW, which is higher than in Case 2 and Case 3. This outcome is expected, as prioritizing high-SV nodes may result in slightly more LS at less vulnerable nodes to maintain overall equity. Specifically, nodes 1, 2, 3, 26, and 28 experienced full load shedding, as they are positioned at the ends of feeders and have relatively low social vulnerability indices. The total cost in Case 1 was $13.55 million, the lowest among all cases, primarily due to a strategic preference for flood mitigation strategies over wildfire mitigation. Since flood mitigation is significantly cheaper ($200,000/mile) than wildfire mitigation ($3 million/mile), the optimization naturally selected reinforcements in flood-prone areas where many high-SV nodes are located. This is evident in the reinforcement of L79-40, L30-29, L50-54, and L74-49, where flood-resistant strategies accounted for 9.69% of the total cost, reducing overall expenditures compared to wildfire mitigation as shown in Table 5. Although lines L3-2, L5-4, and L2-1 are associated with high hazard probabilities, they were not all selected for reinforcement in Case 1. This is due to their location at the ends of feeders and their relatively low load and social vulnerability scores. The optimization model considers not only hazard probability but also the system-level impact of reinforcement, including load served, SV index, cost of mitigation, and contribution to overall network equity. As a result, the model may choose to reinforce lower-risk lines that serve critical or high-SV nodes instead of high-risk lines with limited system impact. This trade-off is consistent with the framework's risk-based goal of achieving balanced performance across cost, resilience, and energy justice. The equity index of 5.1, the highest among all cases, indicates that load shedding and outage durations were distributed most evenly across the network, ensuring a fairer outcome for vulnerable populations. The average outage time in Case 1 is 2.15 h, slightly higher than in Case 2, but significantly lower than the 16.1 h observed in Case 3. Although Case 1 does not achieve the lowest total load shedding or the shortest outage duration, this reflects a deliberate trade-off made by the optimization model. By prioritizing high-SV nodes, the model allows limited shedding at less vulnerable nodes to maintain overall equity. At the same time,

the model achieves the lowest total cost by leveraging more affordable flood mitigation strategies. This balanced result demonstrates the strength of a multi-objective optimization approach that integrates energy justice, enabling cost-effective resilience improvements while ensuring fair treatment across the service area.

Table 5. Investment details by scenario of Case 1. Abbreviations: UG—Undergrounding; FH—Flood-hardening; mi—mile.

Scenario	Type	Lines Reinforced	Length (mi)	Cost (USD)	% Total
1	UG	L32-31	1.09	3,270,000	24
2	UG	L5-4	1.98	5,940,000	44
3	UG	L49-50	1.01	3,030,000	22
4	FH	L79-40, L30-29, L50-54, L74-49	6.57	1,314,000	10
Total	–	–	**10.65**	**13,554,000**	**100**

Note: Bold values indicate total aggregated results.

In Case 2, the recognition justice component is removed, meaning that LS is minimized without SV weighting, while distributional justice remains enforced. Without prioritizing socially vulnerable nodes, the optimization more aggressively minimizes LS across the network, leading to a lower total LS of 680.8 kW compared to Case 1. However, this comes at the expense of a significant increase in total cost to $28.1 million, more than twice the cost of Case 1. The higher cost is attributed to the increased reliance on wildfire mitigation strategies, which are significantly more expensive than flood mitigation. Since recognition justice is no longer enforced, optimization no longer prioritizes areas where high-SV nodes exist. Instead, the model selects reinforcements for wildfire-prone lines, which results in increased financial costs. This shift is reflected in the reinforcement of L2-1, L3-2, L5-4, L30-29, L31-29, L31-30, and L32-31, many of which require costly wildfire-resistant infrastructure. The equity index of 4.3, lower than in Case 1, indicates that removing recognition justice resulted in some higher-SV nodes experiencing disproportionate LS. However, the average outage time was reduced to 1.9 h, the shortest among all cases, due to the increased level of infrastructure reinforcement. The nodes experiencing full LS in this case were 26, 28, 51, 53, and 54, highlighting the impact of shifting reinforcement strategies on LS distribution.

In Case 3, both recognition and distributional justice are removed, meaning that the optimization model only minimizes LS and cost, without any fairness constraints. This approach results in the lowest total LS of 655 kW, as power is restored without considering equity metrics. However, this technical efficiency comes at a substantial social cost, as the average outage time increases dramatically to 16.1 h, the highest among all cases. Without distributional justice, some nodes experience severely prolonged outages, while others recover much more quickly. The total cost in Case 3 was $27.13 million, lower than in Case 2 but still significantly higher than in Case 1. Since equity is not enforced, reinforcement decisions are made purely based on minimizing LS and cost trade-offs. This approach led to a reinforcement strategy that did not necessarily favor cheaper flood-resistant solutions, as cost-efficiency was prioritized without equity constraints. Consequently, reinforcements were made to L5-4, L30-29, L31-30, L32-31, L49-50, L50-54, L54-53, L74-49, and L79-40, with an emphasis on reinforcing key network corridors without prioritizing vulnerable populations. The equity index of 4.6, which is lower than Case 1 but higher than Case 2, indicates that while LS was reduced, some nodes were still left with prolonged outages. The nodes experiencing full LS in this scenario were 1, 2, 3, 26, 27, 28, 51, and 53, a larger set than in the other cases, illustrating the uneven distribution of outage durations.

Figure 5 illustrates the comparison of LS across cases and scenarios. Scenario 4 exhibits the lowest LS, as it involves lines serving the middle of the network, which are critical for maintaining system balance. Conversely, Scenario 3 exhibits the highest LS, as the affected lines primarily serve end-of-feeder nodes, which receive lower priority in Cases 1 and 2. Notably, Case 1 does not reinforce L66-65 in Scenario 4, despite its strategic location. This decision is justified by the presence of an alternate substation at node 80, which can serve the entire feeder, maintaining balance between cost, resilience, and equity.

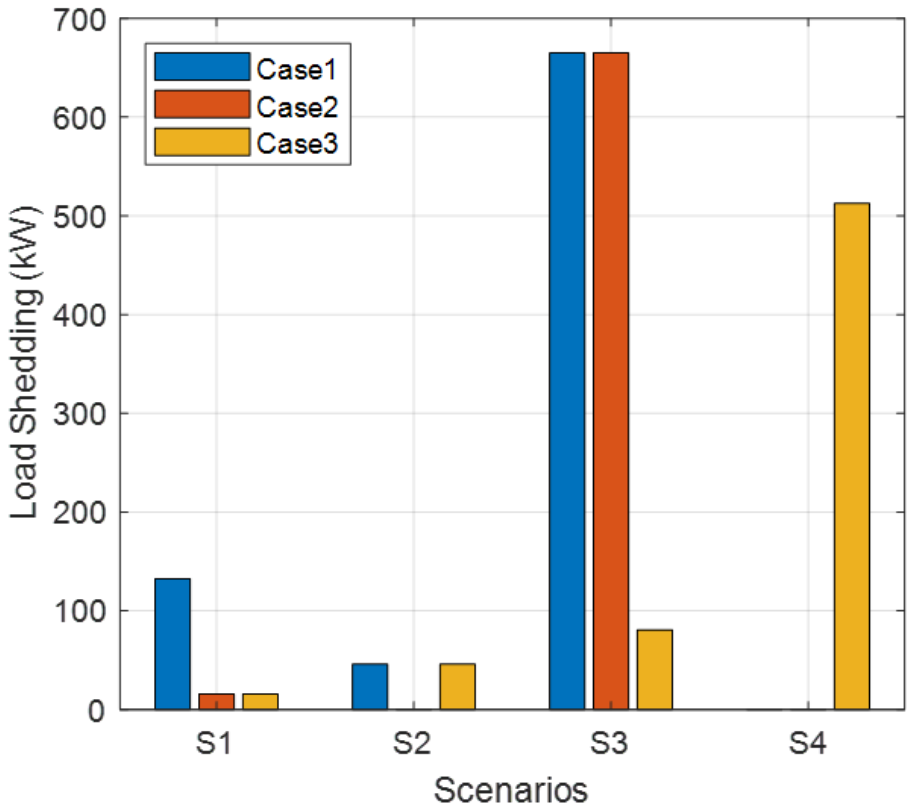


Figure 5. Comparison of Load Shedding Across Cases and Scenarios.

These results highlight the significant impact of incorporating energy justice principles in grid reinforcement planning. Case 1, which enforces both recognition and distributional justice, demonstrates that prioritizing energy justice not only improves equity but also reduces overall cost by leveraging more strategic reinforcement approaches. Conversely, Case 2 results in a higher cost due to increased reliance on wildfire mitigation, while Case 3, which does not consider energy justice, results in the most severe disparities in power restoration. The key insight from this study is that integrating energy justice into optimization models can lead to more socially equitable grid resilience strategies. A general conclusion about the impact of energy justice on reinforcement costs cannot be made however, since it may be impacted by the specifics of the case study, e.g., locations of socially vulnerable populations, the distribution of hazards, and the costs associated with different mitigation strategies.

While the proposed framework demonstrates strong performance in a realistic case study, several assumptions may influence its generalizability. First, the model relies on a DC power flow approximation, which simplifies system behavior by neglecting reactive power and voltage conditions. This approximation is suitable for planning-stage reinforcement studies but can be refined in future work using LinDistFlow or full AC formulations when detailed operational analysis is required or when systems are being studied that are specifically weak in terms of reactive power support. Second, the hazard scenarios

were built using publicly available FEMA and USDA datasets for the Greeley, Colorado area. Applying the model to other regions would require access to localized hazard, cost, and demographic layers to maintain accuracy. Third, the model uses SVI values obtained from census tract data. This level of granularity may not be able to properly handle cases in which multiple feeders, with different vulnerability levels, are all located within the same census tract. More granular socioeconomic data can help refine SVI values in those cases; however, such data may not generally be available or collected with the same level of accuracy as census data. In addition, only capital investment costs were considered in this study, ignoring life cycle impacts and maintenance effects. Finally, although the model converges quickly due to its linear structure, scalability to larger systems will depend on their size, the number of candidate lines, and the number of hazard scenarios. Our assessment indicates that computational complexity scales approximately linearly with the number of scenarios and vulnerable lines, but somewhat nonlinearly with the number of nodes.

5. Conclusions

The growing severity of extreme weather events poses significant challenges to power distribution systems, requiring reinforcement strategies that go beyond traditional cost-driven approaches. This paper introduced a multi-objective optimization framework that enhances grid resilience through hybrid line hardening, considering both technical and societal impacts. The model jointly optimizes resilience, cost, and energy justice to guide equitable and effective reinforcement decisions. Energy justice is captured through recognition and distributional justice: the former prioritizes demand nodes with higher social vulnerability, while the latter ensures equitable distribution of reinforcement benefits. A Chebyshev goal programming method balances conflicting objectives, preventing dominance by any single one.

The framework was applied to a realistic case study of Greeley, CO, under wildfire and flood hazards. Different optimization cases were tested to evaluate trade-offs between objectives. Excluding recognition justice led to higher costs, as more lines were hardened to maintain equity. When both justice elements were excluded, cost and load shedding were minimized, but outage durations became highly unequal. These results show that energy justice can impact reinforcement costs depending on the location of vulnerable populations and hazard exposure, and must be evaluated contextually.

This study emphasizes the need for a holistic grid reinforcement strategy that integrates technical and societal factors. By evaluating multiple objectives, the proposed framework highlights trade-offs between cost, resilience, and equity, offering a structured, scalable approach for prioritizing resilient and just infrastructure investments.

Author Contributions: Conceptualization, A.D. and S.M.; methodology, A.D. and S.M.; software, A.D.; validation, A.D. and S.M.; formal analysis, A.D. and S.M.; investigation, A.D.; data curation, A.D.; writing—original draft preparation, A.D.; writing—review and editing, A.D. and S.M.; visualization, A.D.; supervision, S.M. All authors have read and agreed to the published version of the manuscript.

Funding: This research received no external funding.

Data Availability Statement: Data for this analysis was obtained from publicly available resources as well as data provided in [33].

Conflicts of Interest: The authors declare no conflict of interest.

Nomenclature

Indices and sets

D	Set of all demand nodes in the system, $D \subseteq N$.
f	Index used for the objective functions in the multi-objective framework.
G	Set of all generation nodes in the system, $G \subseteq N$.
h	Index used for hazard types.
H	Set of all hazards considered.
i, j	General indices used to indicate nodes.
L	Set of all lines in the system.
L_v	Set of lines that are vulnerable and hence, candidates for hardening, $L_v \subseteq L$.
N	Set of all nodes in the system.
s	Index used for contingency scenarios.
S	Set of all contingency scenarios.
t	Index used for time.
T	Time horizon of the problem.

Parameters

$b_{i,j}$	Susceptance of the line between nodes i and j [p.u].
c_h	Cost of hardening power line between two nodes for hazard h [$/mile].
$l_{i,j}$	Length of the overhead line between nodes i and j [Mile].
$\overline{P}_{i,j,t}$	Maximum power that can flow through the line connecting nodes i and j at time t [kW]. In the most general case, the maximum power can be a function of time to indicate adjustments such as dynamic thermal rating.
$P^d_{i,t}$	Desired demand at demand node i at time t [kW].
$\overline{P}^g_{i,t}$	Maximum permissible production level for generator at node i at time t [kW]. In the most general case, it can be a function of time, for instance, governed by weather conditions.
$\underline{P}^g_{i,t}$	Minimum permissible production level for generator at node i at time t [kW]. In the most general case, it can be a function of time, for instance, due to technical or contractual constraints.
$p_{h,s}$	Probability of occurrence of contingency scenario s under hazard h.
S_{base}	Base power [kVA].
SV_d	Social vulnerability index for demand node d. A value between 0 and 1, with higher values indicating higher vulnerability levels against long-duration power outages.
$v_{i,j,h,s}$	Binary parameter indicating whether the line connected between nodes i and j is able to operate during scenario s of hazard h, i.e., is immune against that scenario (1: is immune, 0: is vulnerable).
Y_{base}	Base admittance [S].
$\bar{\delta}$	Maximum permissible node phase angle [rad].
T_f	Target value for objective function f in the multi-objective framework.

Variables

$m_{i,t,h,s}$	Binary variable indicating if power delivered to node i at time t under scenario s of hazard h is less than desired.
$n_{i,t,h,s}$	Binary variable indicating if power delivered to node i at time t under scenario s of hazard h meets the desired amount.
$p_{i,j,t,h,s}$	Power flowing through line connecting nodes i and j, at time t under scenario s of hazard h [kW].
$p^d_{i,t,h,s}$	Power demand at node i at time t under scenario s of hazard h [kW].
$p^g_{i,t,h,s}$	Power generation at node i at time t under scenario s of hazard h [kW].
$s_{i,j,h,s}$	Binary variable indicating the overall status of the line connected between nodes i and j during scenario s of hazard h (1: is immune, 0: is vulnerable). Overall status is dependent on the combination of the original vulnerability level of the line against scenario s and whether or not it is hardened.

$u_{i,j,h}$	Binary variable indicating whether the line connected between nodes i and j is considered for hardening against hazard h (1: considered, 0: not considered). Different hardening strategies may be used; for instance, undergrounding lines is considered for resilience against wildfire risks, whereas flood resilience is achieved by using steel or concrete poles and/or strengthening foundations.
$\delta_{i,t,h,s}$	Phase angle at node i at time t under scenario s of hazard h [rad].
b_f	Deficiency variable associated with objective function f in the multi-objective framework.
Q	Maximum deviation of the multi-objective functions from their target values.
O_f	Optimal value for objective function f in the multi-objective optimization framework.

References

1. FERC, NERC and Regional Entity Staff Report: The February 2021 Freeze. Available online: https://www.ferc.gov/news-events/news/final-report-february-2021-freeze-underscores-winterization-recommendations (accessed on 18 January 2025).
2. Hurricane Ian: DOE Situation Update. Available online: https://www.energy.gov/sites/default/files/2022-10/Ian_DOE%20Situation%20Update_9.pdf (accessed on 18 January 2025).
3. 2021 Marshall Fire: Report and Summary of Impacts. Available online: https://mars.colorado.gov/MarshallFire (accessed on 18 January 2025).
4. Keeping the Lights on in Our Neighborhoods During Power Outages. Available online: https://www.energy.gov/gdo/articles/keeping-lights-our-neighborhoods-during-power-outages#:~:text=According%20to%20Climate%20Central%20%2C%20about,impacts%20communities%20across%20the%20country (accessed on 14 April 2024).
5. Federal Energy Regulatory Commission (FERC). Grid Reliability and Resilience Pricing. Federal Register. 2017. Available online: https://www.federalregister.gov/documents/2017/10/16/2017-22215/grid-reliability-and-resilience-pricing (accessed on 31 January 2024).
6. Panteli, M.; Trakas, D.N.; Mancarella, P.; Hatziargyriou, N.D. Power Systems Resilience Assessment: Hardening and Smart Operational Enhancement Strategies. *Proc. IEEE* **2017**, *105*, 1202–1213. [CrossRef]
7. Daeli, A.; Mohagheghi, S. Power Grid Infrastructural Resilience Against Extreme Events. *Energies* **2023**, *16*, 64. [CrossRef]
8. Davarikia, H.; Barati, M. A Tri-Level Programming Model for Attack-Resilient Control of Power Grids. *J. Mod. Power Syst. Clean Energy* **2018**, *6*, 918–929. [CrossRef]
9. Tan, Y.; Das, A.K.; Arabshahi, P.; Kirschen, D.S. Distribution Systems Hardening Against Natural Disasters. *IEEE Trans. Power Syst.* **2018**, *33*, 6849–6860. [CrossRef]
10. Zhou, J.; Coit, D.W.; Felder, F.A.; Tsianikas, S. Combined Optimization of System Reliability Improvement and Resilience with Mixed Cascading Failures in Dependent Network Systems. *Reliab. Eng. Syst. Saf.* **2023**, *237*, 109376. [CrossRef]
11. Haghshenas, M.; Hooshmand, R.A.; Gholipour, M. Power Distribution System Resilience Enhancement Planning Against Extreme Dust Storms via Pre- and Post-Event Actions Considering Uncertainties. *Sustain. Cities Soc.* **2022**, *78*, 103626. [CrossRef]
12. Najafi, J.; Peiravi, A.; Guerrero, J.M. Power Distribution System Improvement Planning Under Hurricanes Based on a New Resilience Index. *Sustain. Cities Soc.* **2018**, *39*, 592–604. [CrossRef]
13. Moglen, R.L.; Barth, J.; Gupta, S.; Kawai, E.; Klise, K.; Leibowicz, B.D. A Nexus Approach to Infrastructure Resilience Planning under Uncertainty. *Reliab. Eng. Syst. Saf.* **2023**, *230*, 108931. [CrossRef]
14. Talebi, S.; Vakilian, M.; Bahrami, M.; Lehtonen, M. Equipment Hardening Strategies to Improve Distribution System Resilience against Wildfire. In Proceedings of the 2022 International Conference on Smart Energy Systems and Technologies (SEST), Eindhoven, The Netherlands, 5–7 September 2022; pp. 1–6. [CrossRef]
15. Ma, S.; Su, L.; Wang, Z.; Qiu, F.; Guo, G. Resilience Enhancement of Distribution Grids Against Extreme Weather Events. *IEEE Trans. Power Syst.* **2018**, *33*, 4842–4853. [CrossRef]
16. Ma, S.; Li, S.; Wang, Z.; Qiu, F. Resilience-Oriented Design of Distribution Systems. *IEEE Trans. Power Syst.* **2019**, *34*, 2880–2891. [CrossRef]
17. Wang, X.; Shahidehpour, M.; Jiang, C.; Li, Z. Resilience Enhancement Strategies for Power Distribution Network Coupled with Urban Transportation System. *IEEE Trans. Smart Grid* **2019**, *10*, 4068–4079. [CrossRef]
18. Hou, H.; Tang, J.; Zhang, Z.; Wang, Z.; Wei, R.; Wang, L.; He, H.; Wu, X. Resilience Enhancement of Distribution Network Under Typhoon Disaster Based on Two-Stage Stochastic Programming. *Appl. Energy* **2023**, *338*, 120892. [CrossRef]
19. Zadsar, M.; Ansari, M.; Ameli, A.; Abazari, A.; Ghafouri, M. A Two-Stage Framework for Coordination of Preventive and Corrective Resiliency Enhancement Strategies in Power and Gas Distribution Systems. *Int. J. Electr. Power Energy Syst.* **2023**, *148*, 108914. [CrossRef]
20. Shen, Y.; Wang, G.; Zhu, J. Resilience Improvement Model of Distribution Network Based on Two-Stage Robust Optimization. *Electr. Power Syst. Res.* **2023**, *223*, 109559. [CrossRef]

21. Shi, Q.; Li, F.; Kuruganti, T.; Olama, M.M.; Dong, J.; Wang, X.; Winstead, C. Resilience-Oriented DG Siting and Sizing Considering Stochastic Scenario Reduction. *IEEE Trans. Power Syst.* **2021**, *36*, 3715–3727. [CrossRef]
22. Pashiri, N.T.; Azad, S.; Ameli, M.T. Distribution system resilience improvement against hurricanes: Optimal line hardening according to reconfiguration potentials. *J. Eng.* **2024**, *2024*, e12364. [CrossRef]
23. Faramarzi, D.; Rastegar, H.; Riahy, G.H.; Doagou-Mojarrad, H. A Three-Stage Hybrid Stochastic/IGDT Framework for Resilience-Oriented Distribution Network Planning. *Int. J. Electr. Power Energy Syst.* **2023**, *146*, 108738. [CrossRef]
24. Wang, J.; Li, Z.; Qian, T.; Tang, W. An Improved Robust Optimization Method for Resilient Distribution Networks with the Strategies of Line Hardening and Distributed Generator Placement. In Proceedings of the 2022 7th Asia Conference on Power and Electrical Engineering (ACPEE), Virtual, 16–17 April 2022; pp. 95–101. [CrossRef]
25. Behzadi, S.; Bagheri, A. A trade-off between line hardening and dynamic line rating by a new convex optimization model for resilient micro-grid-oriented expansion planning of reconfigurable smart distribution networks incorporated with renewable energy sources. *Next Energy* **2025**, *8*, 100351. [CrossRef]
26. Haghshenas, M.; Hooshmand, R.A.; Gholipour, M. Stochastic Planning of Resilience Enhancement for Electric Power Distribution Systems against Extreme Dust Storms. *Iran. J. Electr. Comput. Eng.* **2022**, *20*, 108–120.
27. Ghasemi, M.; Gilani, M.; Amirioun, M. Resilient Gas Dependency–Based Planning of Electricity Distribution Systems Considering Energy Storage Systems. *Risk Anal.* **2024**, *45*, 1716–1728. [CrossRef]
28. Zhang, H.; Ma, S.; Ding, T.; Lin, Y.; Shahidehpour, M. Multi-Stage Multi-Zone Defender-Attacker-Defender Model for Optimal Resilience Strategy with Distribution Line Hardening and Energy Storage System Deployment. *IEEE Trans. Smart Grid* **2021**, *12*, 1194–1205. [CrossRef]
29. Daeli, A.; Dugan, J.; Mohagheghi, S. Optimal Line Hardening in Distribution Systems for Resilience Against Extreme Weather Events. In Proceedings of the 2024 IEEE Industry Applications Society Annual Meeting (IAS), Phoenix, AZ, USA, 20–24 October 2024; pp. 1–7. [CrossRef]
30. Dugan, J.; Byles, D.; Mohagheghi, S. Social Vulnerability to Long-Duration Power Outages. *Int. J. Disaster Risk Reduct.* **2023**, *85*, 103501. [CrossRef]
31. Zhang, J.; He, Y. Fast Solving Method for Two-Stage Multi-Period Robust Optimization of Active and Reactive Power Coordination in Active Distribution Networks. *IEEE Access* **2023**, *11*, 30208–30222. [CrossRef]
32. Jones, D.; Tamiz, M. *Practical Goal Programming*; Springer: New York, NY, USA, 2010; Volume 141. [CrossRef]
33. Sexauer, J.M. Development of Probabilistic Load Flow for Voltage Quality in the Presence of Distributed Generation. Ph.D. Thesis, Colorado School of Mines, Golden, CO, USA, 2012. Available online: https://repository.mines.edu/bitstream/handle/11124/170568/T6996.pdf?sequence=1&isAllowed=y (accessed on 31 January 2024).
34. RES 1 Baseline Load Shape Study Prepared for: The Electric and Gas Program Administrators of Massachusetts. 2018. Available online: https://ma-eeac.org/wp-content/uploads/RES-1-FINAL-Comprehensive-Report-2018-07-27.pdf (accessed on 31 January 2024).
35. Souto, L.; Santoso, S. Overhead versus Underground: Designing Power Lines for Resilient, Cost-Effective Distribution Networks Under Windstorms. In Proceedings of the 2020 Resilience Week (RWS), Salt Lake City, UT, USA, 19–23 October 2020; pp. 113–118. [CrossRef]
36. Climate. Colorado Wildfire Risk Public Viewer. Available online: https://climate.colorado.gov/colorado-wildfire-risk-public-viewer (accessed on 31 January 2024).
37. Weld County. Weld County Property Portal. 2025. Available online: https://gishub.weldgov.com/pages/interactive-maps (accessed on 20 January 2025).
38. AMPL Optimization: Empowering Businesses and Institutions. 2024. Available online: https://ampl.com/ (accessed on 8 April 2024).
39. The Leader in Decision Intelligence Technology—Gurobi Optimization. Available online: https://www.gurobi.com/ (accessed on 27 September 2025).

Disclaimer/Publisher's Note: The statements, opinions and data contained in all publications are solely those of the individual author(s) and contributor(s) and not of MDPI and/or the editor(s). MDPI and/or the editor(s) disclaim responsibility for any injury to people or property resulting from any ideas, methods, instructions or products referred to in the content.